CHEMISTRY OF MATERIALS

Article

pubs.acs.org/cm

Pristine Polysulfone Networks as a Class of Polysulfide-Derived High-Performance Functional Materials

Maciej Podgórski,[†,‡] Chen Wang,[†] Ye Yuan,[§] Danielle Konetski,[†] Ivan Smalyukh,[§] and Christopher N. Bowman*[,†]

[†]Department of Chemical and Biological Engineering, University of Colorado, 3415 Colorado Avenue, JSC Biotech Building, Boulder, Colorado 80309, United States

[‡]Department of Polymer Chemistry, Faculty of Chemistry, Maria Curie-Sklodowska University, Gliniana Street 33, 20-614 Lublin, Poland

[§]Department of Physics, University of Colorado, 2000 Colorado Avenue, Boulder, Colorado 80309, United States

Supporting Information

ABSTRACT: Polysulfide network oxidative modification is presented. Fundamental differences between the properties of sufide-based and sulfone-based networks are discussed, and a method for producing the sulfone-based materials from thioether-based materials is developed. Oxidation enables significant mechanical property enhancements of polysulfide materials without any deleterious effects that typically accompany cross-linking polymerizations. Various application examples such as sulfide-containing particle modification and hardening of soft lithography or thiol−ene 3D microprinted objects are also shown.

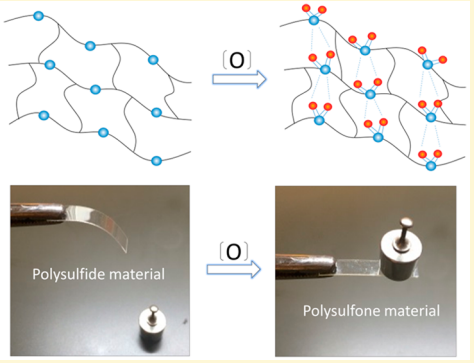

INTRODUCTION

Various postpolymerization modification (PPM) techniques are frequently employed to produce materials with desired properties that would be difficult or impossible to obtain through a conventional polymerization of neat monomers.[1] In other words, these modification methods serve to circumvent effectively the difficulties that arise in direct polymer synthesis. As a whole, the PPM approach constitutes an important polymerization supplementing tool in many interdisciplinary materials science fields as it enables a variety of exciting innovations. Although PPM reactions are most frequently applied to linear polymer chain ends or backbones, there are also multiple examples of network surface or bulk modifications as those known in polymer gels or hydrogels.[2−4] Click reactions are one obvious choice in postpolymerization functionalization of diverse macromolecular substrates. Among them, the thiol-X reaction family has become increasingly dominant. The thiol-X couplings owe their usefulness to high reaction efficiency, mild reaction conditions, the library of unexpansive substrates to choose from, and last but not least, the possibility of triggering the coupling by light (e.g., by radical thiol−ene reactions). Owing to these attributes, the most common implementations in various synthetic approaches involve biofunctionalization,[5−9] substrate or polymer surface functionalization,[8,10−17] and network forming polymerization.[18−23] Within the broad field of research on polymeric networks, significant interest has been dedicated to the synthesis and application of hydrogels,[19,20,24] the development of dental restorative composites,[21,25,26] the preparation of micro- and nanoparticles,[27−30] and nanoimprint and soft lithography techniques.[12,31−35]

One limitation that often arises from the presence of the flexible thioether linkages in the thiol−ene (or thiol-Michael) networks is their rubbery nature, which prevents them from implementation in numerous applications that necessitate more mechanically and thermally robust polymer networks that are common, e.g., for methacrylate- or acrylate-based materials. Further, the lack of toughness and durability of sulfide-based materials is also a limiting factor even in otherwise suitable applications.

A variety of different approaches has been undertaken to circumvent these limitations. Sulfide-based, high modulus networks have been recently synthesized based on ester-free thiol−ene formulations.[36−38] However, polymerization of such mixtures inherently encompasses some of the same drawbacks arising from chain polymerizations in cross-linking systems, namely considerable shrinkage stress and limited functional group conversions. In other reports, thiol-Michael resins incorporating vinyl sulfone monomers were shown to exhibit increased glass transition temperatures as compared to structurally similar thiol−acrylate compositions.[36,39] Still, the

Received: May 19, 2016
Revised: June 23, 2016
Published: June 23, 2016

DOI: 10.1021/acs.chemmater.6b02026
Chem. Mater. 2016, 28, 5102−5109

Table 1. Extent of Sulfide Oxidation within Thiol−ene and Thiol-Michael Networks after 24 h of Peroxide Solution Treatment[a]

thiol/vinyl (1/1)	theoretical/measured mass increase ($S \rightarrow SO_2$) [%]	sulfide oxidation extent [%]	T_g of polysulfide network [°C]	T_g of polysulfone network [°C]
HDT/TTT	20.2/20.3	100	23 (1)	126 (1)
HDT/TMPTA	18.4/14.5	79	−23 (1)	45 (1)
TMPTMP/TTT	14.8/14.2	96	42 (2)	124 (1)
TMPTMP/TMPTA	13.8/13.6	99	4 (2)	62 (1)
PETMP/TEGDVE	14.3/11.9	83	−23 (2)	30 (0)
TMPTMP/DVS	16.6/−		17 (1)	193+
TTTSH/TTT	16.0/14.3	89	80 (1)	202 (2)

[a]Accompanied are the changes in glass transition temperatures (T_g) before and after polysulfide network oxidation. Standard deviation values are included in the brackets.

effect of the sulfone presence was always assessed in networks containing both thioethers and sulfones, among other functional groups, and therefore there has been no direct comparison between the neat sulfide and sulfone materials, let alone any means for systematically converting one into the other. As linear polysulfones are known to be tough materials of high thermal resistance,[40,41] we hypothesized that pristine sulfone networks would also exhibit similarly superior characteristics.

Further, from the standpoint of current applications of sulfide network polymers there exists a reasonable demand for a convenient means of postpolymerization modification of the well-defined but soft thiol−ene/Michael materials to produce structurally uniform and durable materials. Once this goal is accomplished, no deleterious effects associated with the polymerization step would be observed, and the final material would exhibit the oft desired toughness and/or high glassy modulus.

It is well-known that sulfides are conveniently converted into sulfones in solution by oxidation. Performing oxidation in a network would allow the primary structure of the network, as characterized by its cross-linking density and the molecular weight between cross-links, to remain largely unchanged, thus preserving its well-defined, ideal conformation. As the oxidation is very efficient for small molecule compounds, herein, we chose to investigate approaches to sulfide oxidation within a network structure as well as assessment of the advantageous effects of the sulfone presence on the network mechanical properties. In the course of this study, we detail the evolution and the drastic transition in thermo-mechanical properties achievable in polysulfide thiol-Michael as well as thiol−ene network polymers that undergo gradual-to-complete sulfide oxidation. Further, we show relevant application examples of our oxidative methodology that fits perfectly for postpolymerization modification of soft lithography 3D patterns, sulfide-based step-growth microparticles, and other 3D-printed features such as those known, e.g. in stereolitography and microfluidics.

EXPERIMENTAL SECTION

Materials. Dibutyl sulfide, dipropyl sulfide, hydrogen peroxide solution (30%), triallyl-1,3,5-triazine-2,4,6-(1H,3H,5H)-trione (TTT), 2,2,6,6-tetramethylpiperidine 1-oxyl (TEMPO), trimethylolpropane tris(3-mercaptopropionate) (TMPTMP), 1,3,5-tris(3-mercaptopropyl)-1,3,5-triazine-2,4,6-trione (TTT-SH), Trimethylolpropane triacrylate (TMPTA), triethylamine (TEA), pentaerythritol tetra(3-mercaptopropionate) (PETMP), 1,6-hexandithiol (HDT), tri(ethylene glycol) divinyl ether (TEGDVE), divinyl sulfone (DVS) were purchased from Sigma-Aldrich and Bruno Bock, or synthesized in lab.

Polysulfide Oxidation. The polysulfide films were prepared by casting in glass molds. The thiol−ene photopolymers were cured in the presence of 1 wt % Irgacure 651 with UV light (365 nm) of the irradiance intensity of 50 mW/cm^2. The thiol-Michael films were cured thermally with 1 wt % TEMPO (or 2 wt % TEA) at 120 °C for 1 h. The samples of the dimensions 10/4/0.5 or 10/4/0.25 mm were oxidized by immersion in 30% aqueous hydrogen peroxide for 24 h, or less. The samples were dried on hot plate until constant mass at 120−200 °C. The oxidation extent was evaluated by weighting the samples afterward.

Characterization Methods. Fourier transform infrared spectroscopy (Nicolet 6700 FT-IR) was utilized to analyze the polysulfide and polysulfone films. ATR-IR as well as transmission IR were implemented to assess the quality of the oxidized samples.

NMR spectra were recorded on a Bruker Avance-III 400 NMR spectrometer at 25 °C in d-chloroform. Chemical shifts are reported in parts per million (ppm) relative to tetramethylsilane (TMS).

A DMA Q800 (TA Instruments) and was utilized to measure the viscoelastic properties of polymers (glass transition temperature, rubbery storage modulus, tan δ, etc.). Specimens with 0.5 mm × 4 mm × 10 mm rectangular dimensions were tested in multifrequency strain mode by applying a sinusoidal stress of 1 Hz frequency with the temperature ramping at 3 °C min^{-1}. The T_g was determined as the maximum of the tan δ profile. The rubbery moduli were determined in the rubbery region at T_g + 30 °C. T_g half widths were taken as the widths of the tan delta peaks at half-maximum values.

Mechanical properties were measured via a three-point bending test (MTS 858 mini Bionix II). The sample dimensions were 0.5 mm × 5 mm × 20 mm.

X-ray photoelectron spectroscopy (XPS) was implemented to determine the film composition. A PHI 5600 instrument (RBD Instruments) with a monochromatic Al Kα source (1486.6 eV) was used. Survey scans were obtained with a pass energy of 93.9 eV and a step size of 0.400 eV. An electron beam neutralizer was kept on during the measurements. Data was collected with the AugerScan software package (RBD Instruments) and analyzed by the Casa XPS software package (Casa Software).

Contact liquid photolithographic polymerization technique was used to prepare thiol−ene micrometer-sized features. A collimated UV light of the irradiance intensity of 50 mW/cm^2 (365 nm) was shone through a photomask mounted over the liquid mixture of monomers mixed in a stoichiometric ratio of both complementary functional groups. Different photomasks with 5, 10, and 100 μm strips or circles separated by 500 or 100 μm screening gaps were used. Surface topography of the litographic samples was determined using stylus profilometry (Dektak 200VSi stylus profilometer, Veeco).

The two photon polymerization (TPP) setup consisted of a tunable (680−1080 nm) femtosecond pulsed titanium:sapphire laser (Chameleon Ultra-II, Coherent), piezo-electric positioning stage (Physic Instrumente, model P-611.3SF) and a shutter (Uniblitz, model LS3Z2), and a home-built microscope with an oil-immersion objective (100×, numerical aperture NA = 1.4). The average laser power used was around 10 mW and the photopolymerization was done by tuning the laser to 780 nm to optimize two-photon absorption. Shapes of different objects were described by parametric equations programmed

DOI: 10.1021/acs.chemmater.6b02026
Chem. Mater. 2016, 28, 5102−5109

in LabView. The computer-controlled nanopositioning stage changes the relative 3D position of the sample with respect to the focal point of the focused femtosecond laser beam. Laser beam intensity and its polarization direction in the sample are controlled by a half-wave plate and a Glan laser polarizer. In order to impose a computer-generated 3D-shape into the photocurable resin, we continuously translate the stage and time the shutter so that the focus of the femtosecond laser beam can visit and sequentially polymerize all points of the desired volume of the complex-shaped microparticle. Details of this home-built TPP experimental setup and polymerization procedures can be found elsewhere.[42,43]

Nanoindentation tests were performed on a Nanoindenter XP (MTS Systems Corp, Oak Ridge, TN). Details can be found in the SI.

RESULTS AND DISCUSSION

To oxidize sulfides a selection of conventional oxidants have been used, often together with additional catalytic compounds.[44−48] Various metallic complexes facilitate efficient oxidation that can be completed, even in near stoichiometric conditions, in time scales on the order of minutes. Herein, however, a simplified methodology has been initially assessed and later implemented for bulk network oxidation. Specifically, two sulfide compounds, i.e., dipropyl and dibutyl sulfide, were exposed to 4-fold excess hydrogen peroxide (30% in H_2O) in 50/50 vol % solutions with methanol. No other catalytic species were considered. The oxidation extent was analyzed in HNMR experiments in the solutions that were left to react over the course of 1 week at an elevated temperature of 50 °C. This initial study proved that sulfides are completely converted to

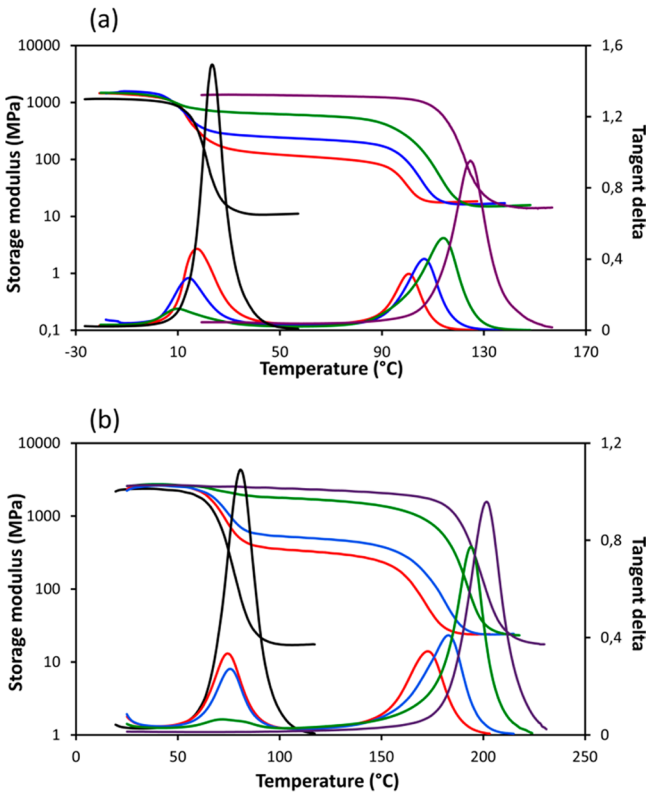

Figure 1. Dynamic mechanical properties of partially and fully oxidized thiol−ene materials: (a) dynamic mechanical analysis (DMA) of HDT/TTT networks oxidized for 30 min (red), 1 h (blue), 2 h (green), and 24 h (purple); (b) DMA data of TTTSH/TTT networks oxidized for 2 h (red), 4 h (blue), 8 h (green), and 20 h (purple). Black curves stand for neat unoxidized thiol−ene samples.

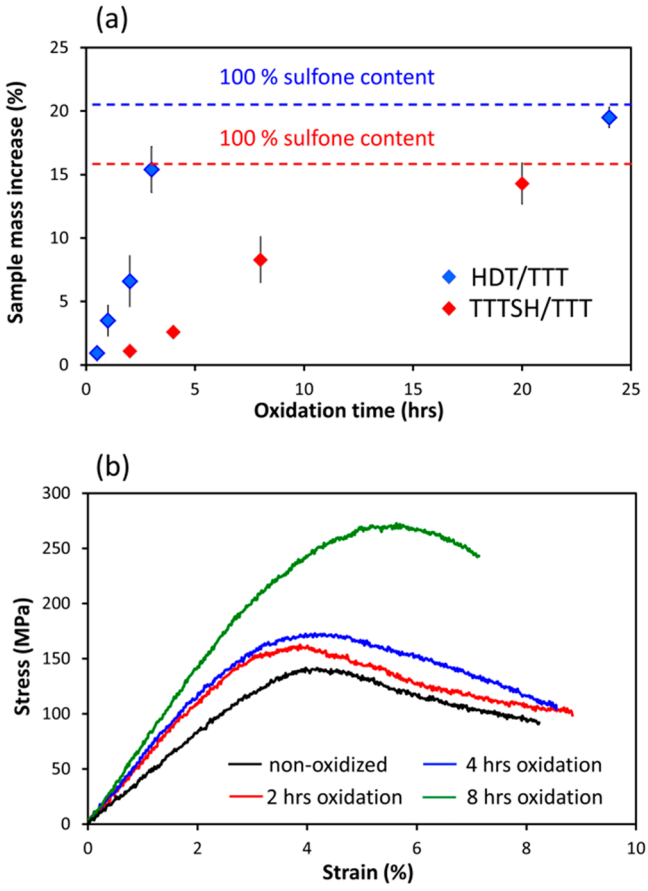

Figure 2. Extent of oxidation and flexural properties of partially and fully oxidized thiol−ene materials: (a) sample mass change during oxidation for HDT/TTT and TTTSH/TTT thiol−ene materials; (b) stress−strain profiles for glassy (T_g 80 °C) thiol−ene TTTSH/TTT material. Black curve stands for neat unoxidized thiol−ene sample.

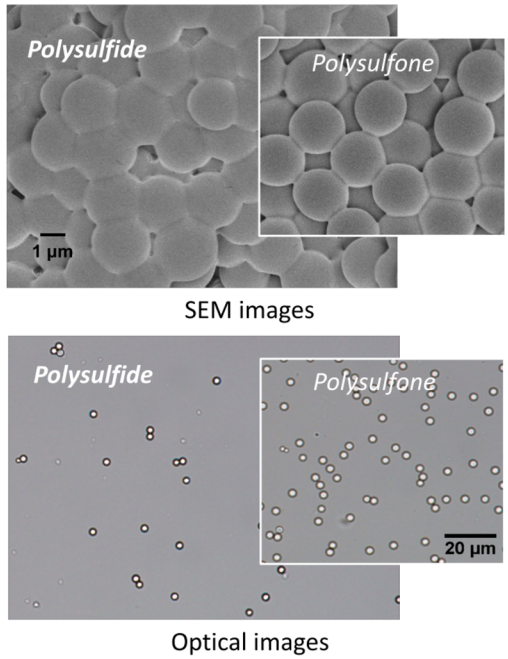

Figure 3. Thiol-Michael particle oxidation SEM and optical images showing no particle geometry change after modification.

DOI: 10.1021/acs.chemmater.6b02026
Chem. Mater. 2016, 28, 5102−5109

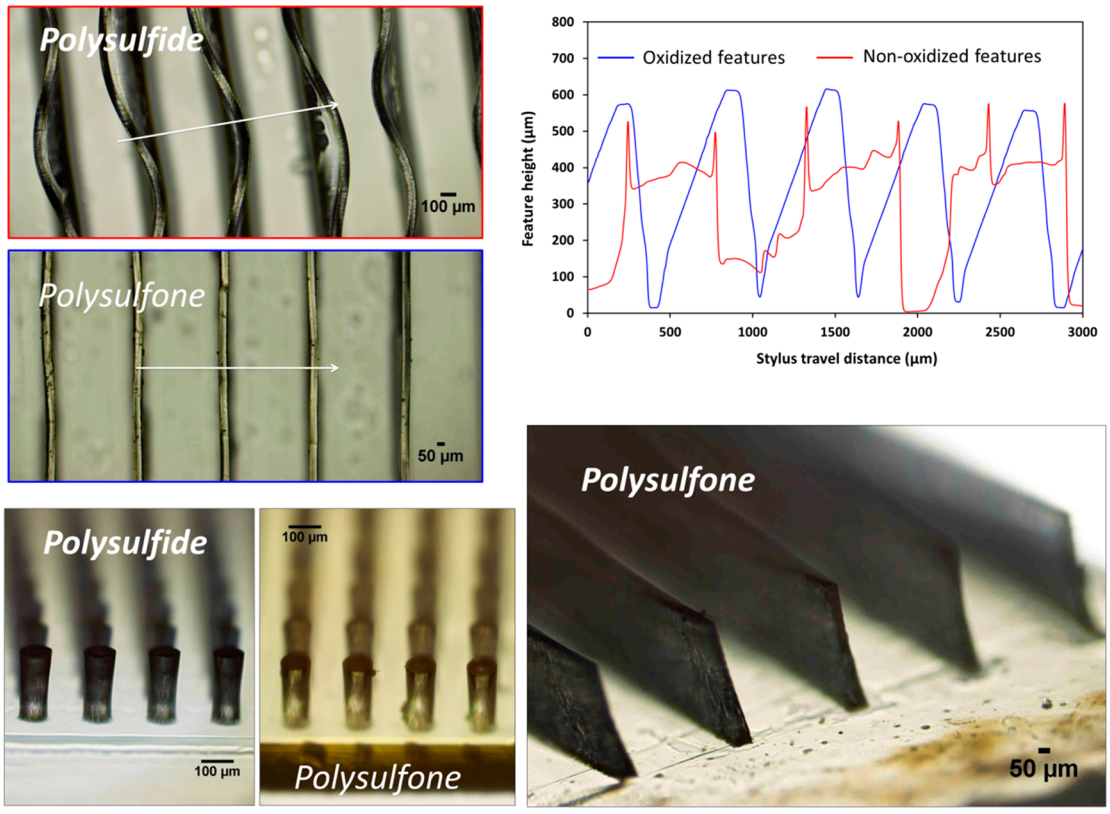

Figure 4. Microscopic images of photopaterned thiol−ene objects (panels and columns) before and after oxidation. Included are profilometry scans on the paneled (nonoxidized and oxidized) structures showing distinctly different profiles.

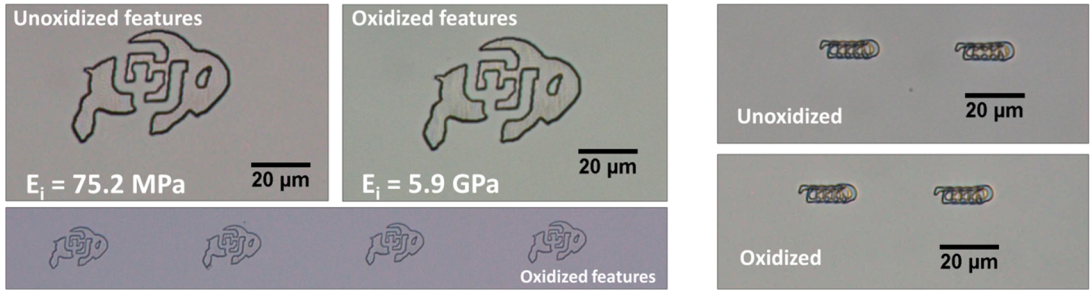

Figure 5. Two-photon polymerized micrometer-sized thiol−ene objects (buffalos and springs) and their nanoindenter moduli (E_i) values. As evidenced in the pictures, drastically different material stiffness can be attained with no discrepancies in object size.

sulfones in diluted hydrogen peroxide solutions (reaction 1), and the first oxidation step, i.e., sulfoxide generation was completed within less than 1 h (Figure S1).

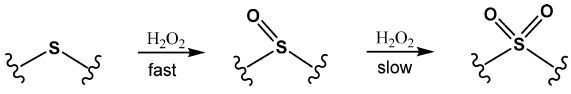

(1)

For sulfide network oxidation, various thiol−ene and thiol-Michael polymeric samples were selected as detailed in Table 1. In our methodology, 250 or 500 μm thick films were exposed to 10−30 wt % hydrogen peroxide for 24 h, washed in acetone and/or DCM, and then dried at elevated temperatures (120−200 °C) until constant weight. Oxidation extent at different time intervals was also analyzed in partially oxidized samples. Sample mass change, transmission IR and ATR-IR analyses, as well as XPS surface studies for some selected specimens were implemented to assess the extent of oxidation. IR and XPS results are presented in SI Figures S2 and S3. As shown in Table 1, all of the analyzed materials were quantitatively (or near-quantitatively) oxidized after 24 h of hydrogen peroxide treatment. The differences between the expected (100% sulfone content) and measured sample weights may originate from the nonideal qualities of the monomers used that may contain leachable impurities. On the other hand, the high temperature drying process may also promote decomposition which is more likely in samples that still contain H_2O_2 as well as sensitive ester moieties. Thorough washing usually prevented any undesired side reactions involving the presence of peroxides.

Interestingly, bulk oxidation, through initial swelling and diffusion of aqueous H_2O_2, is evidently more effective than small molecule oxidation presumably because the thioethers are deprived of unrestricted molecular motions and/or in strained configurations when part of the network. Fixed sulfide positions within a network of high sulfide concentrations make them more accessible to oxidizers whereas strained configurations

DOI: 10.1021/acs.chemmater.6b02026
Chem. Mater. 2016, 28, 5102−5109

may favor electronic rearrangements around sulfur electron free pairs, thus facilitating sulfur−oxygen bond formation. Moreover, the apparent increase in hydrophilicity with the extent of oxidation as observed by Sarapas at al.[49] may also contribute as an adjuvant actuating mechanism and promote faster diffusion/oxidation.

However, the most appealing finding is the material property change observed after oxidation.

As can be seen from Table 1, all specimens exhibit a dramatic increase in glass transition temperatures (T_g). Depending on the initial sulfide content, and the types of monomers incorporated, the resultant polysulfone networks' T_g values were as much as 100 °C higher than the original polysulfide networks. For the first time, these results clearly indicate the fundamental difference between polysulfide and polysulfone network materials. As sulfones are capable of strong electrostatic interactions, it is presumed that large quantities of permanent dipoles evenly distributed throughout the polysulfone networks are contributing immensely to this extraordinary reinforcing effect.

Dynamic mechanical analysis (DMA) was employed to measure the extent and width of thermal transitions as they provide information about structural heterogeneities of the networks.

Additionally, two sets of partially oxidized ester-free thiol−ene samples, consisting of HDT and TTTSH, both reacted with TTT, were analyzed by DMA (Figure 1a,b).

Quantitative oxidation yields polysulfone materials with T_g values of 123 °C for HDT/TTT and 200 °C for TTTSH/TTT, respectively. These values are 100 and 140 °C higher than in the respective thiol−ene networks. Interesting behavior is exhibited by the partially oxidized samples where two transitions regions are clearly observed.

As the oxidation progresses with time, the polysulfide transition gradually disappears in favor of the polysulfoxide/polysulfone transition which becomes dominant and shifts toward higher temperatures. It has been reported that intermediate two-T_g transition materials typically possess triple shape memory properties.[50] Interestingly, the position of the midmodulus plateau is readily controlled here by the extent of oxidation.

The extent of oxidation, as represented by the sample mass increase in the function of oxidation time, is depicted in Figure 2a. As the polymerization of TTTSH and TTT yields a glassy thiol−ene network (T_g = 80 °C), this material was selected for flexural strength testing in the bending configuration mode. Partially oxidized TTTSH/TTT composite samples were analyzed after fixed time intervals in aqueous hydrogen peroxide and the stress−strain plots are included in Figure 2b.

In Figure 2a, it can be seen that the rate of oxidation is dependent on the material cross-linking density. The resin composed of dithiol HDT and triene TTT has a lower rubbery modulus than the more highly functional system (TTTSH/TTT). Additionally, the latter is a glassy material at the oxidation temperature. The swelling, and the reaction itself, is hindered more in TTTSH/TTT, and therefore the overall process requires more time to reach completion. Nevertheless, both materials were completely transformed into polysulfones in less than 24 h of H_2O_2 treatment. Further, the oxidation does not influence the initial cross-link density as the rubbery moduli remained practically unchanged regardless of the oxidation time. Also, the resultant polysulfone networks are characterized by impressive degrees of structural homogeneity which was similar to that of the neat thiol−ene materials. The full-widths-at-half-maximum (fwhm) values for the glass transition span a very narrow range of 20 °C, or even less. Finally, the stress−strain profiles were collected for polysulfide TTTSH/TTT as well as its gradient sulfide/sulfone composite counterparts (Figure 2b). Because it is a hard and structurally homogeneous glass, the pristine thiol−ene system revealed a high flexural strength of 130 MPa.

Moreover, the sulfide/sulfone composite samples showed an increase in flexural strength progressing gradually with the degree of oxidation. After 8 h of oxidation, which was sufficient to convert approximately half of the total amount of network sulfides into sulfones, and/or sulfoxides, the process resulted in a material characterized by an impressive maximal flexural strength of 260 MPa. Fully oxidized samples (not included in Figure 2b) were found to be more brittle, and although possessed higher flexural modulus, their flexural strength amounted to around 220 MPa.

Because of the inherent swelling, and necessary subsequent solvent removal, the proposed network oxidation methodology can be viewed as impractical for modifying thick films, or otherwise large objects. Herein, we describe three application approaches that are suitable for the oxidative modification of functional thiol−ene materials. The current wet modification method can be very efficient for treatment of small three-dimensional objects. As described above, even the oxidation of 500 μm thick films presented no difficulties and resulted in uniform and geometrically flawless materials.

Therefore, a selection of structurally distinct examples, i.e., micrometer-, and sub-micrometer-sized particles, structurally ordered micropatterns, and soft lithography 3D objects, was subjected to oxidation, feature analysis and overall quality assessment.

Recently, we demonstrated the versatility of thiol-Michael cross-linking reactions in the synthesis of monodisperse microspheres.[27,28] By employing a dispersion polymerization method microparticles of diverse sizes and properties were conveniently obtained. Moreover, other recent literature examples also detail new procedures for the synthesis of microparticles as well as nanoparticles based on radically initiated thiol−ene polymerizations.[51,52] Our current oxidation technique enables efficient particle modification by including one additional step in the particle synthesis route. After the completion of the reaction, the step-growth particles are treated with the oxidant while still in the solvent and prior to drying. Particle synthesis/oxidation details are included in the experimental section in the SI. It should be mentioned that any sulfide-containing particles are easily modified by redispersion in an oxidative solvent at any time after polymerization.

Here, we employed a dispersion polymerization technique to prepare and later oxidize sub-micrometer-sized thiol-Michael particles. Trithiol (TMPTMP), divinyl sulfone (DVS) and triethylamine (the catalyst) were used as the reactants. In Figure 3, scanning electron microscopy (SEM) images as well as optical microscopy images of monodisperse microspheres before and after oxidation are presented.

Differential scanning calorimetry (DSC) was used to measure the particles glass transition temperatures.

From the images included in Figure 3, it can be seen that the particles perfectly retain their shape and size after oxidation. On the other hand, the DSC data reveals that soft and rubbery sulfide-containing microbeads (T_g = 8 °C) become hard and

DOI: 10.1021/acs.chemmater.6b02026
Chem. Mater. 2016, 28, 5102−5109

glassy sulfone-materials with T_g significantly higher than 100 °C (Figure S4).

In another application example contact liquid photolithographic polymerization technique was used to fabricate structurally ordered patterns from a photopolymerizable thiol−ene resin. In this approach, a mixture of a trithiol, TMPTMP, and a triene, TTT, deposited on a 250 μm thick TMPTMP/TTT film was irradiated by a collimated UV light through an aligned mask placed on top of the resin. After irradiation, the mask was removed, and the unreacted resin was washed out with ethyl acetate and dried. Two sets of microfeatures, i.e., cylindrical columns with aspect ratio of 2.5:1 and linear panels with aspect ratio of 10:1, were thus prepared and oxidized by immersion in 20% hydrogen peroxide for 1 h (Figure 4).

Additionally, profilometry analysis was performed on the linear patterns perpendicular to their layout direction. As seen from Figure 4, the soft features yield under the moving stylus which results in a ragged and disordered profile whereas the hard features reveal an ordered riblet-like pattern. Because of the high aspect ratio the soft features collapse under their own weight which also results in characteristic wavy lines.

Finally, micrometer-sized 3D structures were created by employing a two-photon polymerization technique (TPP). Similar to the lithographic applications, a TMPTMP/TTT thiol−ene formulation containing UV initiator (0.5 wt %) and radical inhibitor (0.3 wt %) was used. Objects such as horizontal springs and flat buffalo shapes were photopolymerized and subsequently oxidized by hydrogen peroxide solution. Here, a more dilute H_2O_2 solution (15−20% in water) was used to better preserve the faint features on glass substrates and to avoid delamination. A nanoindenter apparatus was chosen to characterize the mechanical properties before and after oxidation. Exemplary images are included in Figure 5.

As seen from the images, there is no trace of any shape distortion to observe after the modification nor any other perceivable differences in shapes or sizes between the oxidized and nonoxidized 3D objects that is discernible. Otherwise identical structures are thus made that differ significantly only in their mechanical properties. The modulus measured for the soft features oscillated around 75 MPa, whereas the hard features yielded a material with nearly 2 orders of magnitude higher modulus at 5.9 GPa.

CONCLUSIONS

In summary, for the first time we demonstrated the fundamental difference between polysulfide and polysulfone network materials as well as a facile conversion method for forming sulfone-containing networks from sulfide-containing networks. As shown, sulfide oxidation is a convenient, clean, and efficient method for the modification of any thioether-based cross-linked material. Small and soft thiol−ene or thiol-Michael objects or features are readily oxidized in bulk to enhance dramatically their mechanical properties without affecting final shapes or sizes. Entirely new high performance sulfone-containing networks were shown to be suitable for applications in the areas such as rapid prototyping, particle synthesis, and soft/imprint lithography.

ASSOCIATED CONTENT

Supporting Information

The Supporting Information is available free of charge on the ACS Publications website at DOI: 10.1021/acs.chemmater.6b02026.

^{1}H NMR and FT-IR spectra, XPS results, DSC plots, nanoindentation results, and particle synthesis details (PDF).

AUTHOR INFORMATION

Corresponding Author

*C. N. Bowman. E-mail: Christopher.Bowman@colorado.edu.

Notes

The authors declare no competing financial interest.

ACKNOWLEDGMENTS

We acknowledge the National Institutes of Health (1U01DE023777-01) and the National Science Foundation (DMR 1420736) for support of this research. We also thank Chelsea Heveran from Prof. Ferguson Lab for nanoindentation measurements.

REFERENCES

(1) Gauthier, M. A.; Gibson, M. I.; Klok, H. Synthesis of Functional Polymers by Post-Polymerization Modification Angewandte. *Angew. Chem., Int. Ed.* **2009**, *48*, 48−58.

(2) Kade, M. J.; Burke, D. J.; Hawker, C. J. The Power of Thiol-Ene Chemistry. *J. Polym. Sci., Part A: Polym. Chem.* **2010**, *48*, 743−750.

(3) Rydholm, A. E.; Bowman, C. N.; Anseth, K. S. Degradable Thiol-Acrylate Photopolymers: Polymerization and Degradation Behavior of an in Situ Forming Biomaterial. *Biomaterials* **2005**, *26*, 4495−4506.

(4) Pei, Y.; Sugita, O. R.; Quek, J. Y.; Roth, P. J.; Lowe, A. B. pH-, Thermo- and Electrolyte-Responsive Polymer Gels Derived from a Well-Defined, RAFT-Synthesized, poly(2-vinyl-4,4-dimethylazlactone) homopolymer via One-Pot Post-Polymerization Modification. *Eur. Polym. J.* **2015**, *62*, 204−213.

(5) Li, M.; De, P.; Li, H.; Sumerlin, B. S. Conjugation of RAFT-Generated Polymers to Proteins by Two Consecutive Thiol−ene Reactions. *Polym. Chem.* **2010**, *1* (6), 854−859.

(6) Jones, M. W.; Gibson, M. I.; Mantovani, G.; Haddleton, D. M. Tunable Thermo-Responsive Polymer−protein Conjugates via a Combination of Nucleophilic Thiol−ene "click" and SET-LRP. *Polym. Chem.* **2011**, *2*, 572−574.

(7) Dondoni, A.; Marra, A. Recent Applications of Thiol−ene Coupling as a Click Process for Glycoconjugation. *Chem. Soc. Rev.* **2012**, *41* (2), 573−586.

(8) Bertin, A.; Schlaad, H. Mild and Versatile (Bio-)functionalization of Glass Surfaces via Thiol-Ene Photochemistry. *Chem. Mater.* **2009**, *21* (24), 5698−5700.

(9) Zou, J.; Hew, C. C.; Themistou, E.; Li, Y.; Chen, C. K.; Alexandridis, P.; Cheng, C. Clicking Well-Defined Biodegradable Nanoparticles and Nanocapsules by UV-Induced Thiol-Ene Cross-Linking in Transparent Miniemulsions. *Adv. Mater.* **2011**, *23* (37), 4274−4277.

(10) Khire, V. S.; Yi, Y.; Clark, N. A.; Bowman, C. N. Formation and Surface Modification of Nanopatterned Thiol-Ene Substrates Using Step and Flash Imprint Lithography. *Adv. Mater.* **2008**, *20* (17), 3308−3313.

(11) Khire, V. S.; Harant, A. W.; Watkins, A. W.; Anseth, K. S.; Bowman, C. N. Ultrathin Patterned Polymer Films on Surfaces Using Thiol-Ene Polymerizations. *Macromolecules* **2006**, *39*, 5081−5086.

(12) Campos, L. M.; Truong, T. T.; Shim, D. E.; Dimitriou, M. D.; Shir, D.; Meinel, I.; Gerbec, J. A.; Hahn, H. T.; Rogers, J. A.; Hawker, C. J. Applications of Photocurable PMMS Thiol-Ene Stamps in Soft Lithography. *Chem. Mater.* **2009**, *21* (21), 5319−5326.

DOI: 10.1021/acs.chemmater.6b02026
Chem. Mater. 2016, 28, 5102−5109

(13) Singha, N. K.; Gibson, M. I.; Koiry, B. P.; Danial, M.; Klok, H. A. Side-Chain Peptide-Synthetic Polymer Conjugates via Tandem "Ester-Amide/thiol-Ene" Post-Polymerization Modification of Poly(pentafluorophenyl Methacrylate) Obtained Using ATRP. *Biomacromolecules* **2011**, *12* (8), 2908−2913.
(14) Mizuno, H.; Buriak, J. M. Catalytic Stamp Lithography for Sub-100 Nm Patterning of Organic Monolayers. *J. Am. Chem. Soc.* **2008**, *130* (52), 17656−17657.
(15) Crowe-Willoughby, J. A.; Genzer, J. Formation and Properties of Responsive Siloxane-Based Polymeric Surfaces with Tunable Surface Reconstruction Kinetics. *Adv. Funct. Mater.* **2009**, *19* (3), 460−469.
(16) Wilderbeek, H. T. A.; Teunissen, J.-P.; Bastiaansen, C. W. M.; Broer, D. J. Patterned Alignment of Liquid Crystals on Selectively Thiol-Functionalized Photo-Orientation Layers. *Adv. Mater.* **2003**, *15* (12), 985−988.
(17) Campos, L. M.; Killops, K. L.; Sakai, R.; Paulusse, J. M. J.; Damiron, D.; Drockenmuller, E.; Messmore, B. W.; Hawker, C. J. Development of Thermal and Photochemical Strategies for Thiol-Ene Click Polymer Functionalization. *Macromolecules* **2008**, *41* (19), 7063−7070.
(18) Kloxin, C. J.; Scott, T. F.; Park, H. Y.; Bowman, C. N. Mechanophotopatterning on a Photoresponsive Elastomer. *Adv. Mater.* **2011**, *23* (17), 1977−1981.
(19) Kloxin, B. A. M.; Kloxin, C. J.; Bowman, C. N.; Anseth, K. S. Mechanical Properties of Cellularly Responsive Hydrogels and Their Experimental Determination. *Adv. Mater.* **2010**, *22*, 3484−3494.
(20) O'Shea, T. M.; Aimetti, A. A.; Kim, E.; Yesilyurt, V.; Langer, R. Synthesis and Characterization of a Library of in-Situ Curing, Nonswelling Ethoxylated Polyol Thiol-Ene Hydrogels for Tailorable Macromolecule Delivery. *Adv. Mater.* **2015**, *27* (1), 65−72.
(21) Carioscia, J. A.; Lu, H.; Stanbury, J. W.; Bowman, C. N. Thiol-Ene Oligomers as Dental Restorative Materials. *Dent. Mater.* **2005**, *21* (12), 1137−1143.
(22) Nair, D. P.; Cramer, N. B.; Scott, T. F.; Bowman, C. N.; Shandas, R. Photopolymerized Thiol-Ene Systems as Shape Memory Polymers. *Polymer* **2010**, *51* (19), 4383−4389.
(23) Ware, T.; Simon, D.; Hearon, K.; Kang, T. H.; Maitland, D. J.; Voit, W. Thiol-Click Chemistries for Responsive Neural Interfaces. *Macromol. Biosci.* **2013**, *13* (12), 1640−1647.
(24) Liu, Z.; Lin, Q.; Sun, Y.; Liu, T.; Bao, C.; Li, F.; Zhu, L. Spatiotemporally Controllable and Cytocompatible Approach Builds 3D Cell Culture Matrix by Photo-Uncaged-Thiol Michael Addition Reaction. *Adv. Mater.* **2014**, *26* (23), 3912−3917.
(25) Boulden, J. E.; Cramer, N. B.; Schreck, K. M.; Couch, C. L.; Bracho-Troconis, C.; Stansbury, J. W.; Bowman, C. N. Thiol-Ene-Methacrylate Composites as Dental Restorative Materials. *Dent. Mater.* **2011**, *27* (3), 267−272.
(26) Beigi, S.; Yeganeh, H.; Atai, M. Evaluation of Fracture Toughness and Mechanical Properties of Ternary Thiol-Ene-Methacrylate Systems as Resin Matrix for Dental Restorative Composites. *Dent. Mater.* **2013**, *29* (7), 777−787.
(27) Wang, C.; Podgórski, M.; Bowman, C. N. Monodisperse Functional Microspheres from Step-Growth "Click" Polymerizations: Preparation, Functionalization and Implementation. *Mater. Horiz.* **2014**, *1* (5), 535−539.
(28) Wang, C.; Chatani, S.; Podgórski, M.; Bowman, C. N. Thiol-Michael Addition Miniemulsion Polymerizations: Functional Nanoparticles and Reactive Latex Films. *Polym. Chem.* **2015**, *6* (20), 3758−3763.
(29) Wang, C.; Zhang, X.; Podgórski, M.; Xi, W.; Shah, P.; Stansbury, J.; Bowman, C. N. Monodispersity/Narrow Polydispersity Cross-Linked Microparticles Prepared by Step-Growth Thiol−Michael Addition Dispersion Polymerizations. *Macromolecules* **2015**, *48* (23), 8461−8470.
(30) Durham, O. Z.; Shipp, D. A. Suspension "click" Polymerizations: Thiol-Ene Polymer Particles Prepared with Natural Gum Stabilizers. *Colloid Polym. Sci.* **2015**, *293* (8), 2385−2394.
(31) Ofir, Y.; Moran, I. W.; Subramani, C.; Carter, K. R.; Rotello, V. M. Nanoimprint Lithography for Functional Three-Dimensional Patterns. *Adv. Mater.* **2010**, *22* (32), 3608−3614.
(32) Moran, I. W.; Briseno, A. L.; Loser, S.; Carter, K. R. Device Fabrication by Easy Soft Imprint Nano-Lithography. *Chem. Mater.* **2008**, *20* (14), 4595−4601.
(33) Carlborg, C. F.; Haraldsson, T.; Oberg, K.; Malkoch, M.; van der Wijngaart, W. Beyond PDMS: Off-Stoichiometry Thiol-Ene (OSTE) Based Soft Lithography for Rapid Prototyping of Microfluidic Devices. *Lab Chip* **2011**, *11* (18), 3136−3147.
(34) Sikanen, T. M.; Lafleur, J. P.; Moilanen, M.-E.; Zhuang, G.; Jensen, T. G.; Kutter, J. P. Fabrication and Bonding of Thiol-Ene-Based Microfluidic Devices. *J. Micromech. Microeng.* **2013**, *23* (3), 037002.
(35) Lin, H.; Wan, X.; Jiang, X.; Wang, Q.; Yin, J. A Nanoimprint Lithography Hybrid Photoresist Based on the Thiol-Ene System. *Adv. Funct. Mater.* **2011**, *21* (15), 2960−2967.
(36) Podgórski, M.; Becka, E.; Chatani, S.; Claudino, M.; Bowman, C. N. Ester-Free Thiol-X Resins: New Materials with Enhanced Mechanical Behavior and Solvent Resistance. *Polym. Chem.* **2015**, *6* (12), 2234−2240.
(37) Podgórski, M.; Becka, E.; Claudino, M.; Flores, A.; Shah, P. K.; Stansbury, J. W.; Bowman, C. N. Ester-Free Thiol−ene Dental restoratives—Part A: Resin Development. *Dent. Mater.* **2015**, *31* (11), 1255−1262.
(38) Podgórski, M.; Becka, E.; Claudino, M.; Flores, A.; Shah, P. K.; Stansbury, J. W.; Bowman, C. N. Ester-Free Thiol-Ene Dental Restoratives-Part B: Composite Development. *Dent. Mater.* **2015**, *31* (11), 1263−1270.
(39) Podgórski, M.; Chatani, S.; Bowman, C. N. Development of Glassy Step-Growth Thiol- Vinyl Sulfone Polymer Networks. *Macromol. Rapid Commun.* **2014**, *35*, 1497−1502.
(40) Nandan, B.; Kandpal, L. D.; Mathur, G. N. Poly(ether Ether Ketone)/poly(aryl Ether Sulphone) Blends: Thermal Degradation Behaviour. *Eur. Polym. J.* **2003**, *39* (1), 193−198.
(41) Sur, G. S.; Sun, H. L.; Lyu, S. G.; Mark, J. E. Synthesis, Structure, Mechanical Properties, and Thermal Stability of Some Polysulfone/organoclay Nanocomposites. *Polymer* **2001**, *42* (24), 9783−9789.
(42) Martinez, A.; Ravnik, M.; Lucero, B.; Visvanathan, R.; Žumer, S.; Smalyukh, I. I. Mutually Tangled Colloidal Knots and Induced Defect Loops in Nematic Fields. *Nat. Mater.* **2014**, *13*, 258−263.
(43) Martinez, A.; Lee, T.; Asavei, T.; Rubinsztein-Dunlop, H.; Smalyukh, I. I. Three-Dimensional Complex-Shaped Photopolymerized Microparticles at Liquid Crystal Interfaces. *Soft Matter* **2012**, *8* (8), 2432−2437.
(44) Sato, K.; Hyodo, M.; Aoki, M.; Zheng, X. Q.; Noyori, R. Oxidation of Sulfides to Sulfoxides and Sulfones with 30% Hydrogen Peroxide under Organic Solvent- and Halogen-Free Conditions. *Tetrahedron* **2001**, *57* (13), 2469−2476.
(45) Legros, J.; Bolm, C. Iron-Catalyzed Asymmetric Sulfide Oxidation with Aqueous Hydrogen Peroxide. *Angew. Chem., Int. Ed.* **2003**, *42* (44), 5487−5489.
(46) Jeyakumar, K.; Chand, D. K. Selective Oxidation of Sulfides to Sulfoxides and Sulfones at Room Temperature Using H2O2 and a Mo(VI) Salt as Catalyst. *Tetrahedron Lett.* **2006**, *47* (27), 4573−4576.
(47) Smith, T. S.; Pecoraro, V. L. Oxidation of Organic Sulfides by Vanadium Haloperoxidase Model Complexes. *Inorg. Chem.* **2002**, *41* (25), 6754−6760.
(48) Bortolini, O.; Di Furia, F.; Modena, G.; Seraglia, R. Metal Catalysis in Oxidation by Peroxides. Sulfide Oxidation and Olefin Epoxidation by Dilute Hydrogen Peroxide Catalyzed by Molybdenum and Tungsten Derivatives under Phase-Transfer Conditions. *J. Org. Chem.* **1985**, *50* (15), 2688−2690.
(49) Sarapas, J. M.; Tew, G. N. Poly(ether-Thioethers) by Thiol-Ene Click and Their Oxidized Analogues as Lithium Polymer Electrolytes. *Macromolecules* **2016**, *49* (4), 1154−1162.
(50) Chatani, S.; Wang, C.; Podgórski, M.; Bowman, C. N. Triple Shape Memory Materials Incorporating Two Distinct Polymer

DOI: 10.1021/acs.chemmater.6b02026
Chem. Mater. 2016, 28, 5102−5109

Networks Formed by Selective Thiol-Michael Addition Reactions. *Macromolecules* **2014**, *47* (15), 4949−4954.
(51) Durham, O. Z.; Norton, H. R.; Shipp, D. A. Functional polymer particles *via* thiol−ene and thiol−yne suspension "click" polymerization. *RSC Adv.* **2015**, *5*, 66757−66766.
(52) Amato, D. V.; Amato, D. N.; Flynt, A. S.; Patton, D. L. Functional, sub-100 nm polymer nanoparticles *via* thiol−ene miniemulsion photopolymerization. *Polym. Chem.* **2015**, *6*, 5625−5632.

DOI: 10.1021/acs.chemmater.6b02026
Chem. Mater. 2016, 28, 5102−5109